Asian Journal of Chemistry; Vol. 30, No. 2 (2018), 421-426

ASIAN JOURNAL OF CHEMISTRY

https://doi.org/10.14233/ajchem.2018.21072

Ultrasonic Behaviour of $CoFe_2O_4 \cdot H_2O$ Magnetic Nanofluids for Magnetic Hyperthermia Applications

V. BEULA SHANTHI AMMANI AMMAL[1], N. JOHN JEBARATHINAM[2] and D. JAYALAKSHMI[3,*]

[1]Department of Physics, Jerusalem College of Engineering, Narayanapuram, Chennai-600 100, India
[2]Department of Chemistry, Jerusalem College of Engineering, Narayanapuram, Chennai-600 100, India
[3]Department of Physics, Queen Mary's College, Chennai-600 004, India

*Corresponding author: E-mail: djayalakshimi2016@gmail.com

Received: 29 September 2017; *Accepted*: 12 November 2017; *Published online*: 31 December 2017; AJC-18717

Cobalt ferrite nanoparticles are prepared by low temperature hydrothermal synthesis using EDTA as template. IR, XRD and FESEM analysis indicate formation of single spinel phase cobalt ferrite particles having average particle size of 26 nm. VSM analysis of cobalt ferrite show hysteresis loop with a moderate coercivity of 580 Oe and saturation magnetization of 60 emu/g. Hyperthermia analysis under various AC magnetic field were carried out for magnetic nanofluids prepared by dispersing various amounts of the synthesized cobalt ferrite nanoparticle in water. The specific absorption rate (SAR) values are found to be comparatively higher for magnetic nanofluids containing cobalt ferrite up to 0.6 wt. % and hence the optimum saturation temperature of 43 °C required for the hyperthermia treatment of cancer cells is achieved by the application of lower magnetic field. Ultrasonic investigation on the prepared nanofluids show no particle-particle interaction up to the concentration of 0.6 wt. % and beyond which agglomeration of particles occur results in the formation of small clusters in the magnetic nanofluids. Presence of clusters reduces SAR values and higher magnetic field is required to attain the optimum saturation temperature of 43 °C.

Keywords: Magnetic nanofluid, Hyperthermia, Ultrasonic studies, Specific absorption rate (SAR), Neel and Brownian movement.

INTRODUCTION

Magnetically tunable nanofluids are most attractive smart materials for technological and biomedical researches and applications [1-3]. Magnetic nanofluids are colloids and considered as a random media in which magnetic nanoparticles are stable and uniformly dispersed in a carrier fluid. When magnetic nanofluids with biocompatible magnetic nanoparticles are injected into a body the magnetic nanoparticles readily bonded with biological entity inside the body and then they can be easily manipulated by external magnetic field gradient. This property of magnetic nanofluids opens up many biomedical applications like drug delivery to the targeted region of the body [4]. Another fascinating behaviour of magnetic nano materials is their capability to generate heat under an alternate magnetic field through hysteresis loss mechanism and Neel and Brownian relaxation mechanism [5,6]. In hysteresis loss mechanism the magnetic nanoparticles with large hysteresis loop area and higher coercivity heated better in presence of high frequency of magnetic field [7]. On the other hand magnetic nanoparticles with zero coercivity (super paramagnetic) undergo Neel and Brownian relaxation mechanisms and get heated in presence of lower frequency of magnetic field [8]. This property of self-heating is the base of a promising application in biomedicine, known as magnetic fluid hyperthermia (MFH) used for the thermal activation therapy of tumor. For this purpose, magnetic nanoparticles in a carrier fluid are placed inside the tumor through direct injection or tumor specific antibody targeting, after which the tumor is exposed to an alternating magnetic field. In earlier days the technical problems associated with hyperthermia are the difficulty of heating only the local tumor to the intended temperature without damaging much of the surrounding healthy tissue and precise control of temperature [9]. In magnetic fluid hyperthermia the above problem can be solved due to the induction heating characteristics of magnetic nanoparticles through the magnetic loss in AC magnetic field. In addition, nanoparticles can be easily transported to the local region of tumor tissue using external magnetic field.

Cobalt ferrite magnetic fluids are found to be best candidate for magnetic fluid hyperthermia applications for achieving the saturation temperature of 43 °C [10,11]. Moreover it is also well established that biocompatible cobalt ferrite nanoparticles can be synthesized by coating with biological molecules [12]. Cano *et al.* [13] studied the degradation rate of cobalt ferrite nanoparticle in a simulated body with and without coating

and the results showed higher stability of both coated and uncoated cobalt ferrite nanoparticles and only less than 0.1 % material lost after 48 h was observed. This small degradation implies that cobalt ferrite nanoparticles can be used in a multifunctional system where first they can be used for drug delivery (duration of 45 h) and subsequently, be used to destroy malignant cells through the hyperthermia process. Many researchers studied the suitability of pure cobalt ferrite and modified cobalt ferrite by replacing Co^{2+} with various divalent ions in the spinel structure for magnetic fluid hyperthermia applications using various liquids as carrier fluid [14-16]. However the behaviour of magnetic nanoparticles in the magnetic fluids at the saturation temperature is still not well established.

The ultrasonic investigations, being non-invasive in nature, highly efficient and relatively low-cost, can provide a powerful means to explore complex colloidal systems like magnetic nanofluids. In late 1970's Chung and Isler [17] studied the application of ultrasound waves to investigate the thermophysical properties of magnetic nanofluids. Followed by this many researchers used the same technique of interaction of acoustic wave with colloidal media for various nanofluids and ferrofluids to study their thermo-physical properties [18,19]. Ultrasonic studies on magnetic nanofluids at various nanoparticle concentration and temperature have been reported in the literature [20,21]. Temperature variation in these studies is done by circulating hot water from a hot water bath. Few reports are also appeared on the variation of ultrasonic parameters under the influence of external magnetic field for cobalt ferrite and magnetite magnetic nanofluids [22,23]. Senthamil Selvi *et al.* [22] reported that colloidal suspensions containing upto 15 wt. % of magnetite particles form small clusters in the presence of an external magnetic field which is attributed to the decrease in ultrasonic velocity. In magnetic fluid hyperthermia applications using cobalt ferrite as magnetic nanofluid, self-heating of nanofluids occurs under the influence of applied AC magnetic field. Hence the state of nanoparticles in the magnetic nanofluid at the saturation temperature is important to know the thermal conductivity of the nanofluid.

In the present investigations, cobalt ferrite nanoparticles are synthesized by low temperature hydrothermal method. Cobalt ferrite nanofluids are then prepared using water as carrier liquid and hyperthermia studies were carried out by applying various AC magnetic field. The saturation temperatures were determined by plotting temperature *versus* time graph and the specific absorption rate (SAR) values were also calculated. Subsequently ultrasonic studies on the cobalt ferrite nanofluid were carried out at saturation temperatures obtained in the hyperthermia analysis in order to understand the state and behaviour of cobalt ferrite nanoparticles in the nanofluid at saturation temperatures.

EXPERIMENTAL

Synthesis of cobalt ferrite: For the synthesis of cobalt ferrite, stoichiometric amounts of AnalaR grade cobalt chloride and ferric chloride in the Co:Fe molar ratio of 1:2 were weighed and dissolved in 50 mL of a solution containing 0.5 g of disodium salt of ethylene diammine tetraacetic acid (EDTA) with constant stirring by magnetic stirrer. 4.4 Molar NaOH solution was added drop by drop into the mixture till the pH is increased to 12. The precipitate produced was stirred for another 3 h at room temperature. Then the precipitate was transferred into an autoclave (23 mL capacity) and kept at a temperature of 120 °C for 12 h in an air oven. The precipitate obtained was centrifuged and washed with distilled water and ethanol.

Hyperthermia studies: Cobalt ferrite nanofluids of different concentrations (0.2, 0.4, 0.6, 0.8 and 1.0 % by weight) were prepared by dispersing specific amount of the synthesized cobalt ferrite nanoparticles in water followed by sonication. Hyperthermia studies were carried out for all the prepared samples under various AC magnetic fields ranging from 15 to 50 mT using EASY HEAT laboratory induction power supply at 250 KHz. During the experiment the coil was cooled to room temperature using a closed loop circulating water system.

Ultrasonic studies: The ultrasonic wave propagation through nanofluid were measured using single frequency (2 MHz) continuous wave ultrasonic interferometer (Modal VCT-70 A, Mittal Enterprises, India) with an accuracy of ± 0.05 % of frequency. Ultrasonic waves are altered by a movable metallic plate kept parallel to the quartz plate. If the separation between these plates is exactly a whole multiple of the sound wavelength, standing waves are formed in the nanofluids. The acoustic resonance gives rise to maximum anode current. The distance between the plates is now increased or decreased, maximum anode current is observed when the variation is half the wavelength or multiple of it. All the prepared cobalt ferrite magnetic nanofluids of concentrations 0.2, 0.4, 0.6, 0.8 and 1.0 wt. % were used for the investigation. Ultrasonic parameters were measured at the saturation temperatures obtained in the hyperthermia analysis of all the samples. The temperature of the sample was maintained using a thermostat and water circulation.

Characterization: Powder X-ray diffraction (XRD) patterns were measured by using RICH-SIEFERT 3000-TT diffractometer employing CuK_α radiation. Fourier transform infrared (FTIR) was performed by the KBr tablet method in the range 4000-250 cm^{-1}, in a BRUKER model IFS 66 V FTIR spectrometer. The morphologies of the samples were examined with field emission scanning electron microscope (FESEM, FEI Nova-Nano SEM-600, The Netherlands). Magnetic measurements were performed by the Quantum design SQUID vibrating sample magnetometer (VSM) at room temperature.

RESULTS AND DISCUSSION

FTIR spectra of the synthesized cobalt ferrite are given in Fig. 1, which shows absorption bands characteristic to spinel structure. The vibrational spectra of absorption bands observed at 330 and 531 cm^{-1} are due to the vibrations of octahedral metal-oxygen bond and tetrahedral metal-oxygen bond respectively. The absence of peaks at 1300-1000 and 3000-2000 cm^{-1} shows non-existence of the O–H mode, C–O mode and C=H stretching-mode of vibrations. This FTIR analysis confirms the method of low temperature hydrothermal synthesis using EDTA as complexing agent results in the formation of pure spinel ferrites.

XRD pattern of the synthesized cobalt ferrite is shown in Fig. 2, which exhibit typical reflections of (220), (311), (222), (400), (422), (511) and (440) planes that are indications of the

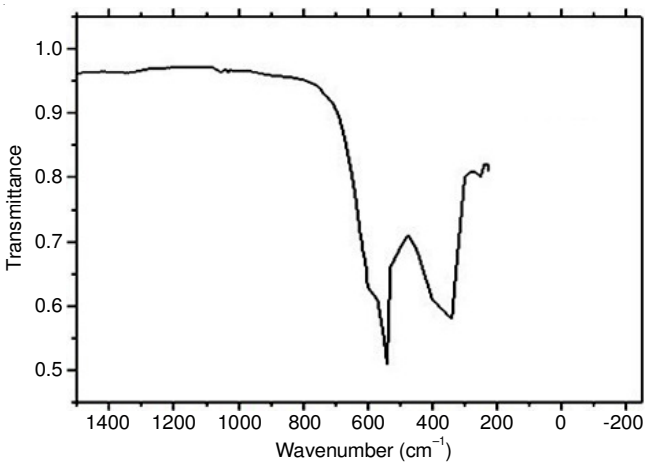

Fig. 1. FTIR spectra of cobalt ferrite

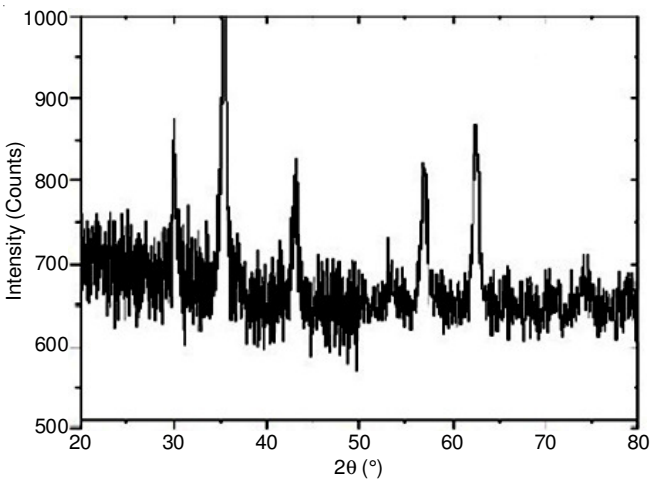

Fig. 2. XRD pattern of cobalt ferrite

presence of the cubic spinel structure. All of the diffraction peaks match well with the reported values (JCPDS file No. 22-1086 for cobalt ferrite). The average crystal size is determined by the Scherrer equation using the peak broadening (FWHM) of the most intense peak (311): $t = 0.9\lambda/\beta\cos\theta$ where λ is the wavelength of CuK_α (1.54059 Å), θ is the angle of Bragg diffraction at full width half maximum (FWHM). The cation distribution at A and B sites are determined by X-ray intensity calculations. The average crystallite size and cation distributions at A and B sites for cobalt ferrite are given in Table-1.

Hyperthermia studies: The induction heating of all the prepared nanofluids (0.2, 0.4, 0.6, 0.8 and 1.0 % wt) in presence of various magnetic fields (15, 25, 40 and 50 mT) are shown in Fig. 3. All the samples show the attainment of saturation temperature at 35 min. Beyond 35 min no significant change in temperature is observed. The saturation temperature obtained for all the cobalt ferrite nanofluids under different magnetic fields are given in Table-2.

It is found that saturation temperature increases with increase of magnetic field at all concentrations (Fig. 4). However the saturation temperature is found to be almost constant up to 0.6 wt. % beyond which it decreases at all magnetic fields (Fig. 5).

Self-heating of magnetic nanofluids is due to any one of the four mechanisms namely eddy currents, hysterises loss, Brownian relaxation and Neel relaxation. Eddy currents contribute significantly only if the particle size is in centimeter scale. For magnetic nanoparticles the other three mechanisms may contribute significantly for self-heating. Cobalt ferrite nanoparticles used in the present investigation are found to have particle size of 26 nm by FESEM analysis (Fig. 6) and also show hysteresis loop with a moderate coercivity of 580 Oe and saturation magnetization of 60 emu/g (Fig. 7). Even though nanoparticles with higher coercivity are heated better to attain the saturation temperature of 43 °C for hyperthermia applications, they require high frequency of external magnetic field. Moreover heating in these nanoparticles is mainly through hysteresis loss mechanism and no significant contribution by Brownian and Neel relaxation which require only low frequency of external magnetic field for induction heating. Since the cobalt ferrite nanoparticles used in the present investigation has only moderate coercivity and small particle size all the three mechanisms may contribute for induction heating.

The saturation temperature of cobalt ferrite nanofluides with concentration of 0.2, 0.4 and 0.6 wt. % are found to be considerably higher compare to the other two samples (0.8 and 1.0 wt. %) under all external magnetic field. Thermal property of magnetic nanofluids are characterized by specific absorption rate (SAR) which is defined as magnetic field energy that is spent for heating per second per unit mass (W/g). The SAR values are calculated using the following equation:

$$SAR = C(\Delta T/\Delta t)\ (1/m)$$

TABLE-1
CRYSTAL PARAMETER AND CATION DISTRIBUTION IN COBALT FERRITE

Sample	Lattice constant (a) (Å)	Volume of unit cell (a^3) (Å^3)	Average size from XRD (nm)	Average size from FESEM (nm)	Cation distribution	
					A site	B site
Cobalt ferrite	8.44	601.21	33.28	26.38	0.25 Co^{2+} 0.75 Fe^{3+}	0.75 Co^{2+} 1.25 Fe^{3+}

TABLE-2
SATURATION TEMPERATUR AND SPECIFIC ABSORPTION RATE (SAR) OF COBALT FERRITE

Field (mT)	0.2 %		0.4 %		0.6 %		0.8 %		1.0 %	
	SAT (°C)	SAR (W/g)	SAT (°C)	SAR (W/g)	SAT (°C)	SAR (W/g)	SAT (°C)	SAR (W/g)	SAT (°C)	SAR (W/g)
15	39.3	99.60	39.2	103.5	39.1	107.0	35.8	82.8	33.2	62.0
25	43.4	120.20	43.2	125.7	43.1	131.6	38.5	96.4	35.3	76.2
40	48.3	140.27	48.1	147.8	48.1	152.6	41.7	109.1	39.4	98.2
50	51.9	160.70	51.1	138.9	50.9	172.4	44.9	132.5	42.9	118.5

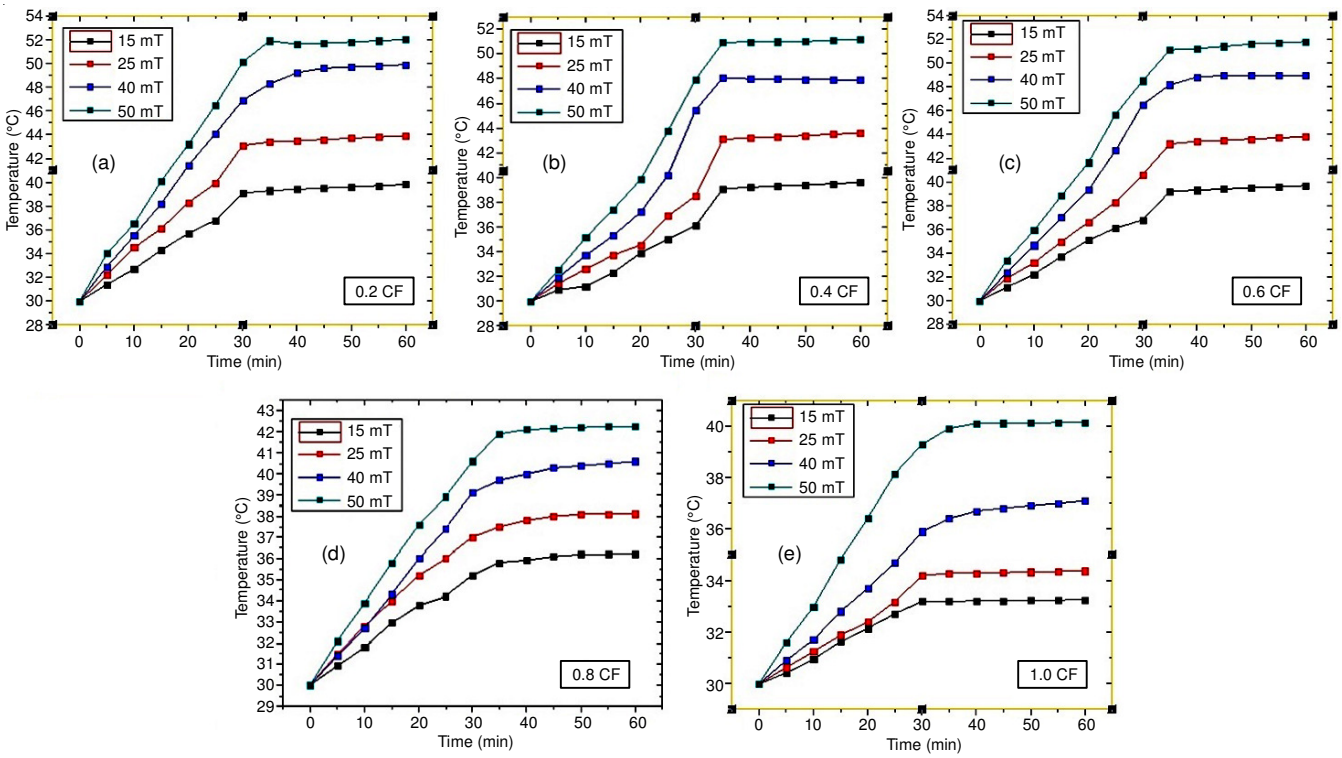

Fig. 3. Hyperthermia analysis of cobalt ferrite nanofluid (a) 0.2, (b) 0.4, (c) 0.6, (d) 0.8 and (e) 1.0 [all in wt. %]

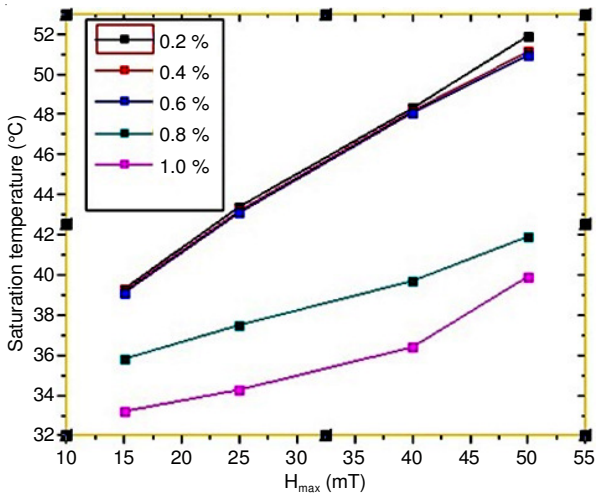

Fig. 4. Effect of magnetic field on saturation temperature

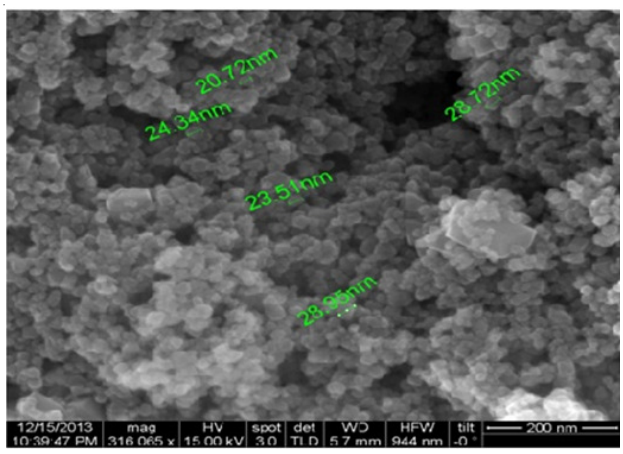

Fig. 6. FESEM analysis of cobalt ferrite

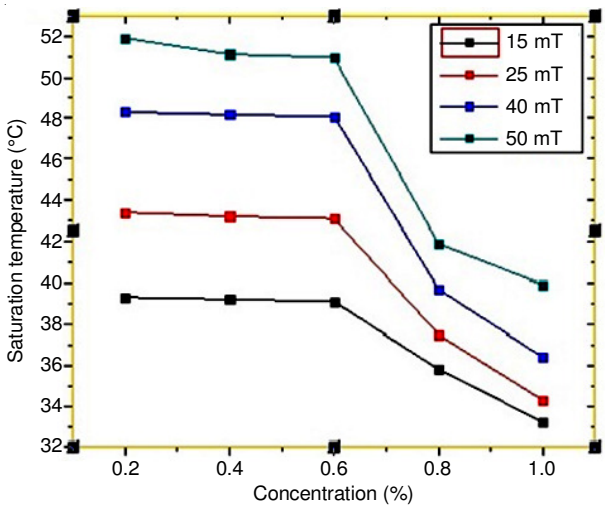

Fig. 5. Effect of concentration on saturation temperature

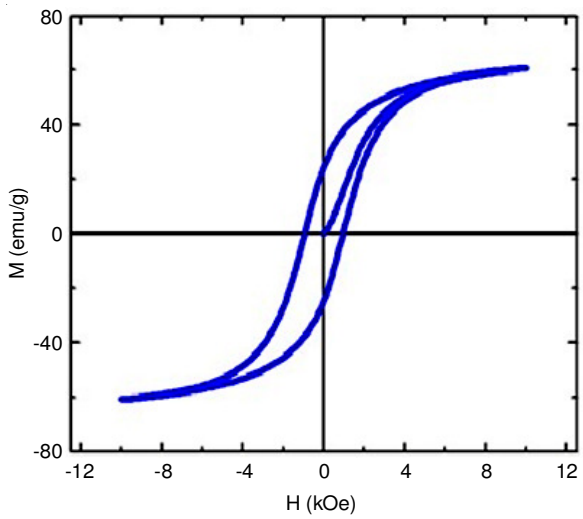

Fig. 7. VSM studies on cobalt Ferrite

where C is the nanofluid's heat capacity, ($\Delta T/\Delta t$) characterizes the temperature change with time, m is a mass of cobalt ferrite in nanofluid. The SAR values calculated for the cobalt ferrite nanofluids at various concentrations under various external magnetic fields are given in Table-2. It is found that the SAR values are increasing with concentrations upto 0.6 % and beyond which it decreases. All the above observations clearly shows that there is a change in the behaviour of cobalt ferrite nanofluids when the concentration of cobalt ferrite nanoparticle is increased above 0.6 % in the carrier fluid water.

Ultrasonic studies: In the hyperthermia analysis even though an AC magnetic field is applied the magnetic nanofluid loses its magnetic characteristics at the saturation temperature and behave like nonmagnetic nanofluid. Moreover Nabeel Rashin and Hemalatha [23] who investigated the effect of magnetic field on the cobalt ferrite nanofluid by ultrasonic studies and reported that when the magnetic field is turned off, the ultrasonic velocity returns to its initial value without exhibiting any hysteresis. Hence the behaviour of cobalt ferrite nano fluid at the saturation temperatures which is attained by applying an external AC magnetic field will be similar to that of cobalt ferrite magnetic nanofluid heated to same temperatures by hot water circulation. The results of hyperthermia analysis shows (Table-2) the saturation temperatures are almost same for cobalt ferrite concentrations of 0.2, 0.4 and 0.6 wt. % under the application of a constant applied AC magnetice field. Hence in the present investigation ultrasonic studies were carried out at temperatures 39.2(312.2 K), 43.2(316.2 K), 48.2(321.2 K) and 51.3 (324.3 K) which are the average saturation temperatures obtained during hyperthermia analysis up to concentration 0.6 wt. %. The ultrasonic velocity (V) inside the nanofluids can be determined using the following equation:

$$V = \lambda f$$

where V is the ultrasonic velocity, λ is wavelength of ultrasound inside the nanofluid and f is the frequency of ultrasonic oscillator (2 MHz). The results are given in Fig. 8(a-c). The ultrasonic velocity [Fig. 8(a)] is found to be almost same with increase in concentration upto 0.6 Wt. % and beyond which it starts decreases. The same trend appears in all saturation temperatures. The adiabatic compressibility (β) and acoustic impedance of the nanofluid medium (Z) are also calculated using the following relations:

$$\beta = 1/\rho V^2$$

$$Z = \rho V$$

where ρ is the density of the nanofluid and V is the ultrasonic velocity. The results obtained are given in Figs. 8(b) and 8(c), respectively. It is found that the results of acoustic impedance show the same pattern as that of ultrasonic velocity [Figs. 8(a) and 8(c)]. But the values obtained for adiabatic compressibility shows the reverse trend [Figs. 8(a) and 8(c)].

In the present investigation water is used as carrier liquid for the preparation of magnetic cobalt ferrite nanofluids. The carrier liquid water has four hydrogen bonds per molecule. The hydrogen bonding pattern in water consists of tetrahedral three-dimensional structures of interacting molecules and form hydrogen bonded clusters which is referred as open structure water. Liquid water also consists of unbounded monomeric water molecules which are occupying space between clusters and these dense molecules are called closed structure water. Fig. 8(a) shows that at a fixed temperature the ultrasonic velocity is found to be almost constant with increase in concentration upto 0.6 wt. %. However the observed values are higher than the ultrasonic velocity of the carrier fluid water. This observation is attributed to the particle-fluid interaction of the individual small size cobalt ferrite nanoparticles on the surface of open and closed structure water molecules. This interaction between particle and fluid may disturb the hydrogen bonding network and causes slight increase in the propagation of ultrasound than the carrier fluid. This trend continues only upto 0.6 wt. % and beyond which as the concentration of nanoparticles increases particle-particle interaction predominates which results in the aggregation of nanoparticles leading to formation of small clusters. The clusters formed are so small that still they are in random motion and interrupt the propagation of sound waves which is accounted for the decrease in ultrasonic velocity beyond the concentration of 0.6 wt. % [Fig. 8(a)].

Ultrasonic investigation confirms no particle-particle interaction in the nanofluids up to cobalt ferrite concentration of 0.6 wt. % at all saturation temperatures. In hyperthermia studies the optimum saturation temperature (43 °C) is attained when the concentration of cobalt ferrite nanoparticles is below 0.6 wt. % (Fig. 3) even in the presence of a lower applied AC magnetic field of 25 mT. Similarly higher SAR values (Table-2) are obtained in presence of lower applied magnetic field for lower concentration (0.2, 0.4 and 0.6 wt. %). These observations indicate contribution of Neel and Brownian relaxations by isolated nanoparticles for induction heating of cobalt ferrite nanoparticles within the concentration of 0.6 wt. %. Above

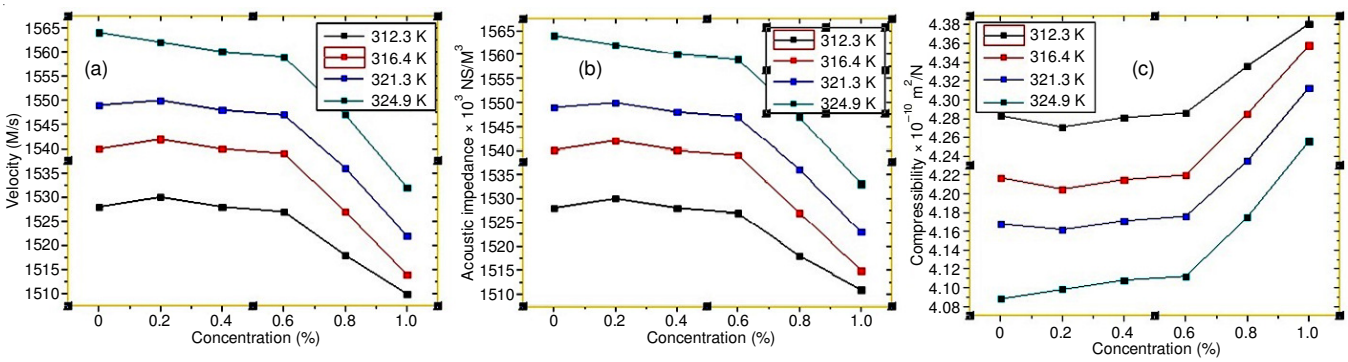

Fig. 8. Ultrasonic studies on cobalt ferrite nano fluid (a) ultrasonic velocity, (b) acoustic impedance and (c) compressibility

0.6 wt. % the saturation temperature decreases and higher magnetic field (50 mT) must be applied in order to achieve the optimum temperature of 43 °C. Ultrasonic investigations establish existence of small clusters above 0.6 wt. % concentrations in the cobalt ferrite nanofluids. Unlike isolated particles clusters of cobalt ferrite nanoparticles can undergo induction heating in presence of AC magnetic field predominantly through hysteresis loop mechanism. As the area of hysteresis loop observed for the cobalt ferrite nanoparticles used in the present investigation are small (Fig. 6), the optimum temperature of 43 °C is achieved by the application of slightly higher magnetic field of 50 mT.

Conclusion

Cobalt ferrite magnetic nanofluids upto concentrations of 0.6 wt. % are found to show no agglomeration of particles by ultrasonic studies. Existence of isolated cobalt ferrite nanoparticles in the cobalt ferrite nanofluids induces induction heating quickly due to higher specific absorption rate (SAR) achieved by Neel and Brownian relaxation mechanisms and the optimum saturation temperature of 43 °C is attained by application of lower magnetic field. Ultrasonic studies also show agglomeration of cobalt ferrite particles above 0.6 wt. % concentration resulting in the formation of small clusters which reduces the SAR value and require higher magnetic field to increase SAR values in order to attain the saturation temperature of 43 °C through induction heating.

ACKNOWLEDGEMENTS

One of the authors, N. John Jebarathinam gratefulto Jawaharlal Nehru Center for Advanced Scientific Research, Bangalore, India for recording FESEM micrograph and VSM analysis of the synthesized samples.

REFERENCES

1. N.A. Hill, *J. Chem. Phys. B*, **104**, 6694 (2000); https://doi.org/10.1021/jp000114x.
2. J. Volatron, J. Kolosnjaj-Tabi, Y. Javed, Q.L. Vuong, Y. Gossuin, S. Neveu, N. Luciani, M. Hémadi, F. Carn, D. Alloyeau and F. Gazeau, *Sci. Rep.*, **7**, 40075 (2017); https://doi.org/10.1038/srep40075.
3. H. Kahil, H.M. El-Sayed, E.M. Elsayed, A.M. Sallam, M. Talaat and A.A. Sattar, *Rom. J. Biophys.*, **25**, 209 (2015).
4. K.A. Sampath, T. Himanshu, B. Kevin and S.P. Singh, *Bioceram. Develop. Appl.*, **6**, 91 (2016); https://doi.org/10.4172/2090-5025.100091.
5. B. Fischer, B. Huke, M. Lücke and R. Hempelmann, *J. Magn. Magn. Mater.*, **289**, 74 (2005); https://doi.org/10.1016/j.jmmm.2004.11.021.
6. A. Gupta and R. Kumar, *Appl. Phys. Lett.*, **91**, 223102 (2007); https://doi.org/10.1063/1.2816903.
7. D. Chowdhury, *Nanoscience Methods*, **1**, 37 (2012); https://doi.org/10.1080/17458080.2010.501459.
8. F.F. Fachini and A.F. Bakuzis, *J. Appl. Phys.*, **108**, 084309 (2010); https://doi.org/10.1063/1.3489983.
9. E. Peng, J. Ding and J.M. Xue, *New J. Chem.*, **38**, 2312 (2012); https://doi.org/10.1039/C3NJ01555F.
10. P. Pradhan, J. Giri, G. Samanta, H.D. Sarma, K.P. Mishra, J. Bellare, R. Banerjee and D. Bahadur, *J. Biomed. Mater. Res.*, **81B**, 12 (2006); https://doi.org/10.1002/Jbm.B.30630.
11. E.L. Verde, G.T. Landi, J.A. Gomes, M.H. Sousa and A.F. Bakuzis, *J. Appl. Phys.*, **111**, 123902 (2012); https://doi.org/10.1063/1.4729271.
12. T. Yadavalli, H. Jain, G. Chandrasekharan and R. Chennakesavulu, *AIP Adv.*, **6**, 055904 (2016); https://doi.org/10.1063/1.4942951.
13. M.E. Cano, R.H. Medina, V.V.A. Fernandez and P.E. Garcia-Casillas, *Rev. Mex. Ing. Quim.*, **13**, 555 (2014).
14. S. Laurent, S. Dutz, U.O. Häfeli and M. Mahmoudi, *Adv. Colloid Interface Sci.*, **166**, 8 (2011); https://doi.org/10.1016/j.cis.2011.04.003.
15. A.E. Deatsch and B.A. Evans, *J. Magn. Magn. Mater.*, **354**, 163 (2014); https://doi.org/10.1016/j.jmmm.2013.11.006.
16. J.-S. Chen, D.R. Poirier, M.A. Damento, L.J. Demer, F. Biancaniello and T.C. Cetas, *Int. Biomed. Morer. Res.*, **22**, 303 (1988); https://doi.org/10.1002/jbm.820220405.
17. D.Y. Chung and W.E. Isler, *J. Appl. Phys.*, **49**, 1809 (1978); https://doi.org/10.1063/1.324819.
18. A. Jozefczak and A. Skumiel, *Czech. J. Phys.*, **54**, D647 (2004); https://doi.org/10.1007/s10582-004-0164-6.
19. K.R. Nemade and S.A. Waghuley, *Indian J. Pure Appl. Phys.*, **53**, 670 (2015).
20. A. Jozefczak, A. Skumiel and P. Regulska, *Mol. Quant. Acoust.*, **25**, 153 (2004).
21. A.V. Rajulu, G. Sreenivasulu And K. S. Raghuraman, *Indian J. Chem. Technol.*, **1**, 302 (1994).
22. C.S. Selvi, C.T. Valliammai, P. Malliga, C. Thenmozhi and V. Kannappan, *Rasayan J. Chem.*, **10**, 271 (2017); https://doi.org/10.7324/RJC.2017.1011605.
23. M.N. Rashin and J. Hemalatha, *Ultrasonics*, **54**, 834 (2014); https://doi.org/10.1016/j.ultras.2013.10.009.